

ANALYSIS OF A TWO BLADED WIND TURBINE UNDER RANDOM LOADING

João Antônio Pires Alves^{a,b}, Rubens Sampaio^a, Henning Spiegelberg^c and Peter Hagedorn^c

^a Pontifícia Universidade Católica do Rio de Janeiro, Rua Marquês de São Vicente, 225 - Gávea - RJ - BRAZIL, <http://www.puc-rio.br>

^b Instituto Nacional de Metrologia, Qualidade e Tecnologia, Av. N. S. das Graças, 50 - Xerem - Duque de Caxias - RJ - BRAZIL, <http://www.inmetro.gov.br>

^c TU Darmstadt, Dynamics & Vibrations Group Dolivostr. 15, 64293 Darmstadt, GERMANY

Keywords: Structural dynamics, propagation of uncertainties, random vibration, eolic energy generation.

Abstract. This work is focused in the study of the dynamic behavior of a two bladed wind turbine, considering random wind loading. The aerodynamic forces actuating over the blades are calculated using a simple approach, assuming that both, the fluctuation of the wind speed incident on the airfoil and pitch angle have a linear relation with the resultant loadings meaning that variations in lift and drag forces can be approximated by an affine transformation at a given point of operation. The nacelle and rotor blades are considered rigid bodies mounted in a flexible tower. All movements, except for the in-plane rotation of the rotor, are considered small so that a linear approach can be applied. Based on this model, the calculation of stochastic stresses in critical spots over the structure is performed.

1 INTRODUCTION

Among the possibilities to extract power from wind movement, surely the first that comes into mind is making the wind to pass through a set of blades connected to a shaft so that a certain amount of energy is transferred from the wind to the blades, making them to move and rotate the shaft. This is sufficient to capture mechanical energy from the wind and this has been done for centuries.

Wind turbines have several configurations but those of interest for this work are installed in the ground and have horizontal axis (see Figure 1). There are three main parts of mechanical interest: The tower that holds the whole structure at a certain height from the ground, the nacelle, where all the mechanical and electro-electronic equipment for the generation and control of energy are housed and, the third part, the rotor which is, in its turn, composed by the shaft, the hub and the blades. In order to transform the mechanical energy in electricity is necessary to couple a generator to the shaft and somehow keep energy stable by controlling the rotor angular velocity. It is quite obvious that the wind direction and magnitude vary quickly and constantly, in both vertical and horizontal plane so that the turbine is almost always misaligned by a certain amount which causes power losses (Veldkamp (2006)). In Figure 1, it is shown the main turbine movements.

The tower is subjected to wind loads indirectly via hub as well as directly when wind blows over its surface. No matter the type, the wind causes to the structure oscillatory movements in several directions which produce torques and forces of random nature. So, knowing the loads acting in the structure and their random responses is of critical importance to determine the structure life and the risk involved in its operation (Veldkamp (2006), Ramirez (2010)).

Two bladed turbines have pros and cons.

- They permit to save 20% to 25% of the total costs of the construction (Spiegelberg (2011), Gasch (2010)) because of the reduced number of blades
- They have a higher rotation so it is good for gearboxes which can be lighter and less expensive
- It is possible to mount the blades on a teeter hub (isolates the low-speed shaft from the out-of-plane bending loads (Andersen (2010)))

but,

- They are noisier and the unfavorable visible appearance of two rotating blades, characterized as "restless" (Spiegelberg (2011), Burton et al. (2001))
- Asymmetry in wind flow causes asymmetric loading moment
- There is a pulsating moment of inertia with respect to a nacelle fixed axis with half turn frequency (Spiegelberg (2011)), (Veldkamp (2006))

The dynamic of a turbine is essentially non-linear as it must be facing the wind all time so adjusting itself rotating the nacelle by a finite angle. Complications are also found when one needs to analyze transient conditions. It is not easy to develop a turbine full model, considering each detail, so simplifications were made in this work. The purpose is to study the movement of a horizontal two bladed turbine under its optimum rotation with small perturbations in- and out-plane due to deterministic and random loading. It is considered that the angle referred as

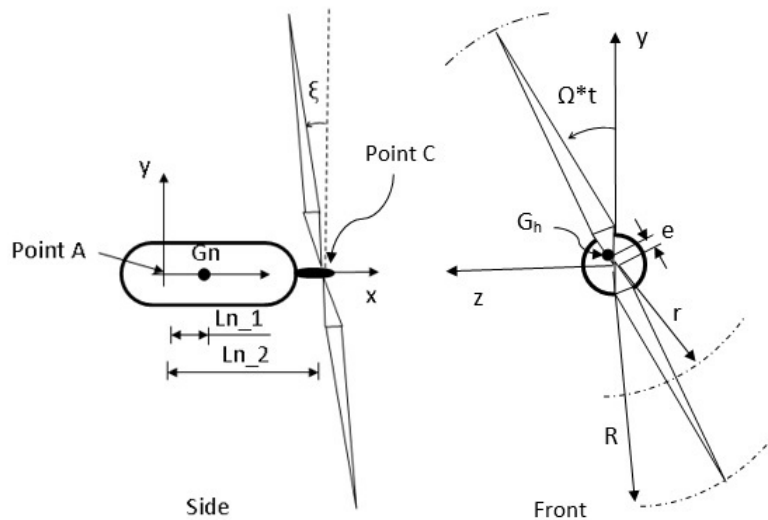


Figure 2: Nacelle and rotor views

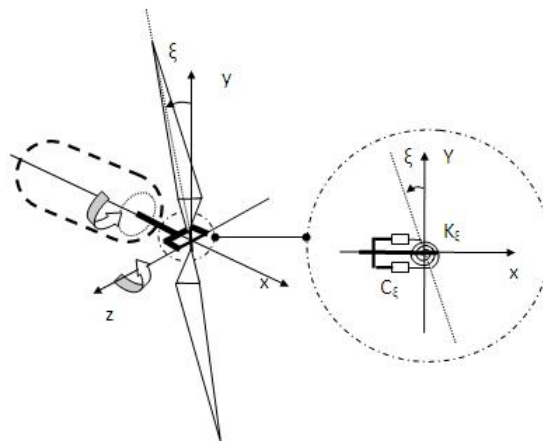


Figure 3: Rotor detail (teetering)

2 LOADS CAUSED BY WIND

The phenomenon of power transmission in wind turbines is intrinsically complex. There are simplified models and one of the simpler is to consider the rotor a permeable disk where some fundamental concepts are obtained in 1D conservative flow, that is, no frictional forces are considered (Actuator Disk Concept). From this approach it is shown that there is a maximum amount of energy that can be extracted from wind (Betz limit) as the wind always exits the turbine with some residual energy. A more sophisticated analysis is possible by using Beam Element Method (BEM). This method permits the association of the momentum theory with localized aspects related to the blade form considering localized interactions between blade and wind. Those both methodologies are treated in (Hansen (2008), Mikkelsen (2003)). The drag and lift forces per unit of length represented in Figure 4 are calculated as a function of \mathbf{W} , the velocity of the wind as seen by the blades, as follows

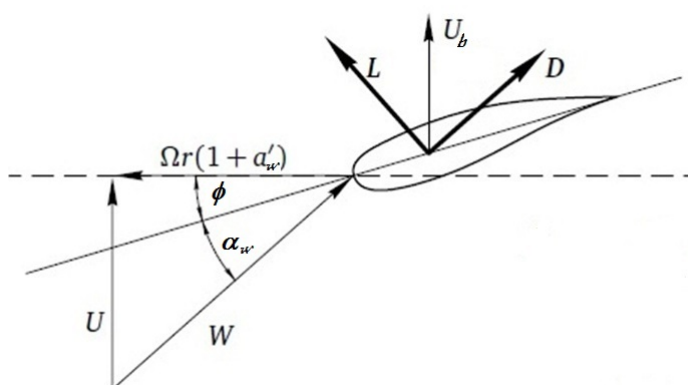


Figure 4: Aerodynamic forces in an airfoil

$$\begin{aligned} L &= \frac{1}{2} \rho_{air} \|\mathbf{W}\|^2 C_L c(r), \\ D &= \frac{1}{2} \rho_{air} \|\mathbf{W}\|^2 C_D c(r), \end{aligned} \quad (1)$$

where ρ_{air} is the air density, $c(r)$ the airfoil local chord length, C_D and C_L are drag and lift local coefficients, respectively. For analyzing the interaction between blade and wind under teetering movement, it can be taking in consideration that the blades move out-plane. The assumption that the teetering angle is small leads to a considerable simplification. In Figure 3, U is the incident wind velocity at the plane of rotation and U_b the out-plane blade velocity. U is the difference between wind flow U_∞ and the axial induced wind (aU_∞ , a is the axial induction factor) plus the increment in velocity due to the actual wind fluctuation U_w and the speed of the blade in axial direction, U_b . As the wind varies in time and space, for obtaining the variation of moments and forces acting on the blades, one must determine the speed \mathbf{W} , the drag and lift coefficients, C_D and C_L , and then integrate the expressions 1 along the rotor radius r , $[0 \leq r \leq R]$ (see Figure 2). This process is however complicated but some simplification can be made, depending on the case. If the rotor is in a given rotation and submitted to a given level of forces, say \bar{L} and \bar{D} , the dynamic about this point may be analyzed considering an affine transformation, resulting from the first order approximation of a Taylor series at the point \bar{L} and \bar{D} (Burton et al. (2001)). In other words, the fluctuations in lift and drag forces about the nominal values are considered small perturbations. This approach takes in consideration that the lift forces dominate out-plane movement, what means that the rotor works with small angles of attack and with high speed ratios ($\lambda = \frac{\Omega R}{U_\infty}$). The varying out-plane forces and moments are, then:

$$\Delta F_{out} = \rho_{air} \Omega \pi \int_{-R}^R U_w(r, \Omega t) c(r) |r| dr, \quad (2)$$

$$\Delta T_{out} = \rho_{air} \Omega \pi \left(\int_{-R}^R U_w(r, \Omega t) c(r) |r| r dr - (\dot{\xi} + \Omega \xi \tan(\delta_3)) m_{\xi_T} \right), \quad (3)$$

with,

$$m_{\xi_T} = 2 \int_0^R c(r) r^3 dr. \quad (4)$$

In equations 2 to 4, r is the position of the point measured from the center of the rotor axis, R is the rotor radius and $c(r)$ is the chord length and r is the distance from the center of rotation

to any point in the blade. The angle δ_3 is imposed in the design. In order to permit the relative out plane rotation between blades and hub it is necessary a hinge or a mechanical linkage. If the hinge is inclined related to the blade axis, out plane angles are coupled to pitch. In this work, $\delta_3 = 0$. It must be mentioned that the term $-\rho_{air}\Omega\pi(\dot{\xi} + \Omega\xi \tan(\delta_3)) m_{\xi_T}$ represents the sum of the aerodynamic stiffness ($-\rho_{air}\Omega^2\pi\xi m_{\xi_T} \tan(\delta_3)$) and the aerodynamic damping $-\rho_{air}\Omega\pi\dot{\xi} m_{\xi_T}$. In the turbine dynamical formulation, those terms appear as external loadings. As the first expression has dependency on ξ it must be incorporated to the stiffness matrix and the second, with dependency on $\dot{\xi}$, must be incorporated to the damping one as can be seen in Annex A.

3 MODELING THE COMPONENTS

The structure for wind power generation is modeled as a set of three bodies, one flexible and two rigid. The flexible one is the tower that holds both, nacelle and rotor, the two rigid bodies. There are three reference systems involved: One inertial, fixed in the ground, one moving system at the top of the tower that is the same as the fixed in nacelle (it does not move relatively to the top of the tower since they are rigidly fixed each other (by hypothesis) meaning that rotational and translational degrees of freedom at point A of the tower and the nacelle are the same) and the last at the intersection between the plane of rotation and shaft (x axis) which rotates with the rotor. A general view of the system is presented in Figure 2. The equations can be obtained in any approach but in this work, they were derived from Euler and Newton laws directly (it is also possible to use the Kane approach (Kane (1985), Spiegelberg (2011))).

The tower was modeled as a Bernoulli-Euler beam submitted to small bending, torsion and normal deformations, although not considering the inertia effects, in a first approximation. The tower is considered to have symmetry along the y axis, so that the equilibrium equations, considering the bending, axial loadings and torsion are uncoupled. Besides, the transversal sections are considered constant as well as its constitutive properties.

3.1 Nacelle and rotor analysis

In the nacelle analysis, two limitations are imposed (see Figure 2):

- The support of the nacelle is at point A
- The center of mass of the nacelle G_n , the point A and the point C are co-linear.

In both rotor and nacelle analysis, the displacements and rotations (except for the rotor rotation in x direction) are considered small so, linearization is possible.

In Figure 5 is presented the degrees of freedom associated to the nacelle. The nacelle is permitted to move in x , y , z directions with displacements u_x , u_y , u_z about the point A and rotations, β about x , α about y and γ about z . It is affected by the rotation of the rotor (due to the wind action in the blades and also to an eventual unbalance) which transmits the loading to the shaft at point C : the moment $\mathbf{M}h_n$ and force $\mathbf{F}h_n$. External moment $\mathbf{M}e_n$ and force $\mathbf{F}e_n$ can be also applied. The movement is constrained by the support reactions (tower) whose moment and force are $\mathbf{T}r_n$ and $\mathbf{F}r_n$, respectively. In principle, the rotations and displacements experienced by the nacelle can be linearized. Of course, when the nacelle is driven to face the wind, α experiences large large values but it is not the case here. In this work, the nacelle is considered to be in a given position under small perturbations. The rotor has a nominal angular velocity with small perturbations in- and out-plane but without any pitch or flapping movement (the only out plane movement in this model is that of the ξ angle). The point C is the connection

between the nacelle and rotor. The Figure 7 to 9 shows the loading acting in the nacelle and rotor.

3.1.1 Nacelle and rotor kinematics

One needs to determine the position of rotor and nacelle center of mass and their orientation in time in order to know their motions. The Figures Figures 5 and 6 show the nacelle and rotor rotation degrees of freedom.

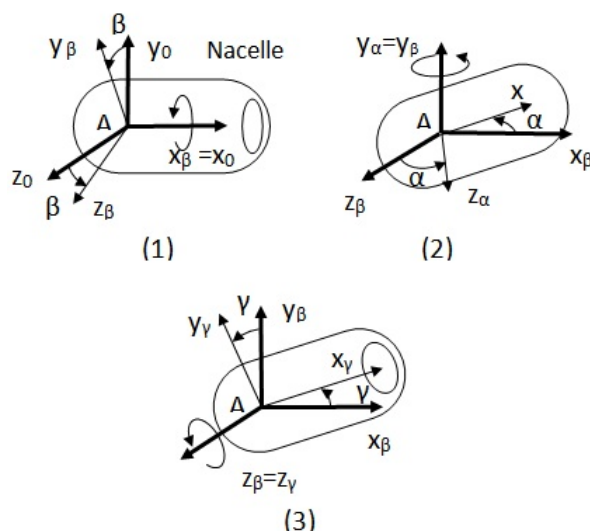


Figure 5: Positioning the nacelle

Related to the nacelle, if the sequence of rotations β , α and γ is applied, the angular velocity and acceleration related to the fixed system 0 can be obtained directly, considering that those rotations are small

$$\varpi_n = \begin{pmatrix} \dot{\beta} \\ \dot{\alpha} \\ \dot{\gamma} \end{pmatrix}, \quad (5)$$

and

$$\ddot{\varpi}_n = \begin{pmatrix} \ddot{\beta} \\ \ddot{\alpha} \\ \ddot{\gamma} \end{pmatrix}. \quad (6)$$

The same principle can be used for the rotor, choosing the sequence ω , ξ . As mentioned before there is not any pitch movement. The rotation ξ remains small so the rotor angular velocity and acceleration, related to a fixed system 0, can be obtained after some algebraical treatment, and are, respectively

$$\varpi_h = \begin{pmatrix} \Omega \\ \dot{\alpha} - \dot{\xi} \sin(\Omega t) \\ \dot{\gamma} + \dot{\xi} \cos(\Omega t) \end{pmatrix}, \quad (7)$$

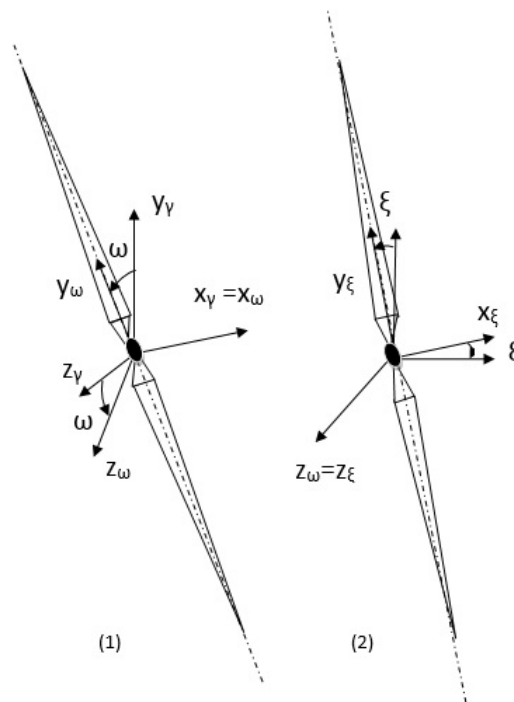


Figure 6: Positioning the rotor

and

$$\ddot{\omega}_h = \begin{pmatrix} 0 \\ \ddot{\alpha} - \ddot{\xi} \sin(\Omega t) - \Omega \dot{\xi} \cos(\Omega t) \\ \ddot{\gamma} + \ddot{\xi} \cos(\Omega t) - \Omega \dot{\xi} \sin(\Omega t) \end{pmatrix}. \quad (8)$$

The nacelle is also permitted to translate. Three more degrees of freedom are defined, u_x , u_y and u_z at point A . So, for the characterization of the nacelle movement, 6 degrees of freedom are necessary. With respect to the rotor, its movement is linked to the nacelle at point C . So, knowing the movement of nacelle means knowing the movement of point C . As the rotation of the rotor is fixed (Ω) and known, the only degree of freedom is ξ .

3.1.2 Nacelle and rotor dynamics

The forces and torques acting in the nacelle are presented in Figure 7. They are,

- \mathbf{T}_e is the external torque,
- \mathbf{T}_t is the torque caused by the reaction of the tower,
- \mathbf{T}_h is the torque caused by the rotor,
- \mathbf{F}_t is the force caused by the tower at point A ,
- \mathbf{F}_e is the external force,
- \mathbf{P}_n is the nacelle weight acting at point G_n .

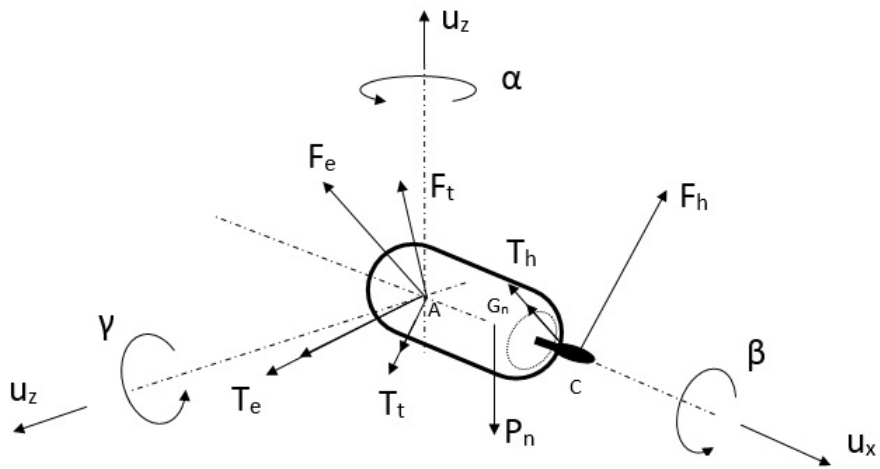


Figure 7: Nacelle forces and torques

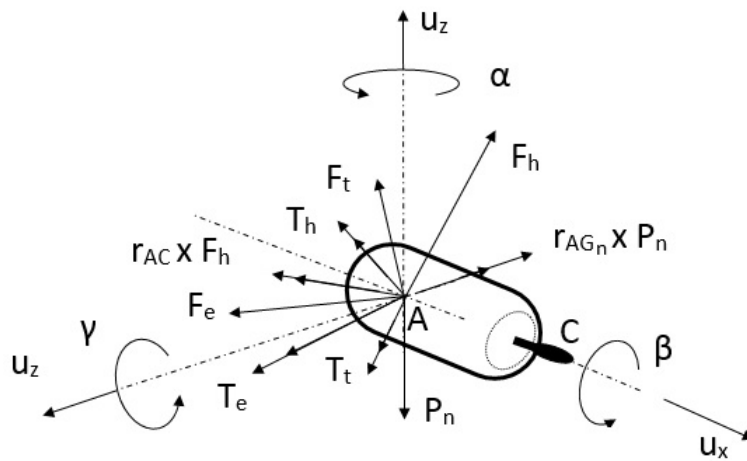


Figure 8: Nacelle equivalent forces and torques

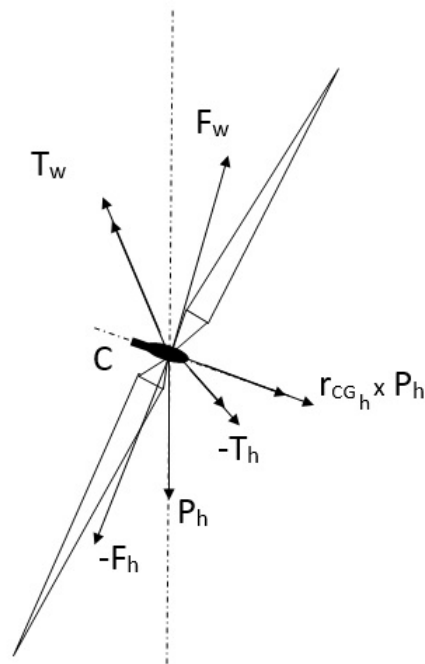


Figure 9: Rotor forces and torques

The forces \mathbf{F}_h and \mathbf{P}_n cause moments in relation to point A , $\mathbf{r}_{AC} \times \mathbf{F}_h$ and $\mathbf{r}_{AG_n} \times \mathbf{P}_n$, respectively. In Figure 8 is shown the equivalent equilibrium with a torque of magnitude $\mathbf{r}_{AC} \times \mathbf{F}_h$ and a force \mathbf{F}_h applied to point A . Considering the rotor, the loading is presented in Figure 9. The force \mathbf{F}_w is due to the wind action as well as the torque \mathbf{T}_w . The weight is not collinear with the point C because of the unbalance causes a moment relative to point C , $\mathbf{r}_{CG_h} \times \mathbf{P}_h$. It is equivalent to a force \mathbf{P}_h acting at point C and a torque with the same magnitude of the referred moment. A force and a moment act in the rotor as a result of the reaction of the nacelle to the rotor movement. They have the same magnitude of \mathbf{F}_h and \mathbf{T}_h , but have opposite directions. From figure 9, the Euler law applied to nacelle is

$$\mathbf{T}_e + \mathbf{T}_t + \mathbf{T}_h + \mathbf{r}_{AC} \times \mathbf{F}_h + \mathbf{r}_{AG_n} \times \mathbf{P}_n = \frac{d}{dt} \mathbf{H}_n^A + \mathbf{r}_{AG_n} \times (m_n \mathbf{a}_n). \quad (9)$$

The second Newton's law is then

$$\mathbf{F}_e + \mathbf{F}_t + \mathbf{F}_h + \mathbf{P}_n = m_n \mathbf{a}_n. \quad (10)$$

Similarly, the Euler's equations for the rotor is

$$\mathbf{T}_w - \mathbf{T}_h + \mathbf{r}_{CG_h} \times \mathbf{P}_h = \frac{d}{dt} \mathbf{H}_h^C + \mathbf{r}_{CG_h} \times (m_h \mathbf{a}_h). \quad (11)$$

and for the Newton's law

$$\mathbf{F}_w - \mathbf{F}_h + \mathbf{P}_h = m_h \mathbf{a}_h. \quad (12)$$

Combining the two equations, (9) and (11), one obtains

$$\begin{aligned} \mathbf{T}_e + \mathbf{T}_t + \mathbf{T}_w + \mathbf{r}_{AC} \times \mathbf{F}_h + \mathbf{r}_{AG_n} \times \mathbf{P}_n + \mathbf{r}_{CG_h} \times \mathbf{P}_h = \\ \frac{d}{dt} \mathbf{H}_n^A + \mathbf{r}_{AG_n} \times (m_n \mathbf{a}_n) + \frac{d}{dt} \mathbf{H}_h^C + \mathbf{r}_{CG_h} \times (m_h \mathbf{a}_h). \end{aligned} \quad (13)$$

Similarly, combining equations 10 and 12 one obtains, for the force equilibrium

$$\mathbf{F}_e + \mathbf{F}_t + \mathbf{F}_w + \mathbf{P}_n + \mathbf{P}_h = m_n \mathbf{a}_n + m_h \mathbf{a}_h. \quad (14)$$

Equations 13 and 14 form six differential equations that involve seven degree of freedom represented in vector Ψ below:

$$\Psi = \begin{pmatrix} \beta \\ \alpha \\ \gamma \\ \xi \\ u_x \\ u_y \\ u_z \end{pmatrix}. \quad (15)$$

By coupling a stiffness and dissipation system between shaft and hub it is possible to keep the rotation ξ under limits. The out-plane torque due to the wind action in the blades is partially responsible to the change of the angular momentum of the rotor and it is possible to find this quantity by formulating the rotor equilibrium from the point of view of the rotative coordinated system coupled to the rotor. The torque T_w due to the wind action is then, in this rotating system, represented as a vector with constant direction as well as ξ and its local derivatives. The same happens with the reaction of the stiffness and dumping system, whose resultant is parallel to T_w but points towards opposite direction. Writing the Euler law to the rotor one more equation is obtained, similar to 13. So, the system now can be solved for Ψ .

Obtaining the seven equations represented by 13, 14 is quite exhaustive and the help of an applicative for manipulating symbolic equations is of good use. The resultant seven equations are grouped in a system as represented below

$$\mathbf{P} = [M]\ddot{\Psi} + [D]\dot{\Psi} + [K]\Psi. \quad (16)$$

In equation 16, $[M]$, $[D]$ and $[K]$ are the matrices mass, dumping and stiffness, respectively and are presented in 7. \mathbf{P} is the loading vector and Ψ is the vector containing the degrees of freedom, as shown in equation 15.

4 DYNAMIC OF THE TURBINE AND THE COLUMN TOGETHER

Although more accurate approach can be employed to model the tower, e.g., using FEM and/or modal analysis, in this work a much simpler model will be used instead. The tower will be considered a Bernoulli-Euler beam without dynamic effects so that the final movement can be obtained in a closed way. The angular and axial displacements at the top of the tower will be obtained as a function of the forces and torques acting at the top of the tower. This is a system of algebraic equations whose degrees of freedom are the rotations and displacements at the top. Combining this system with the equations of 16, the tower influence is incorporated to the nacelle/turbine equilibrium. From elementary elasticity analysis (Shigley (1978)), if shear forces and torques are acting the top of a tower, as presented in Figure 10, they can be written as functions of the angular and linear displacements (at the top). These torques, forces, displacements and angles will be made compatible with those of the nacelle already formulated in equation 16. One considers the bending in two planes, xy and yz . The displacement on the top due to the forces and torques are, in x and z directions

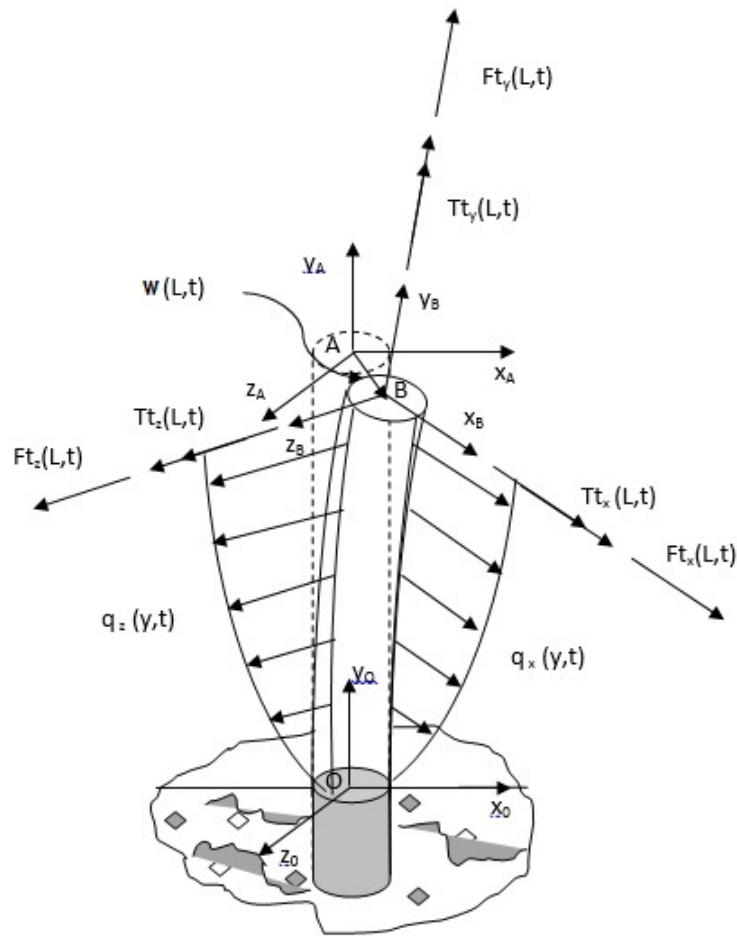


Figure 10: Loads in the tower

$$\begin{aligned} w_x &= a_1 * Ft_x - b_1 Tt_z, \\ w_z &= a_1 * Ft_z + b_1 Tt_x, \end{aligned} \quad (17)$$

Similarly, the angle on the top due to the forces and torques are, in x and z directions

$$\begin{aligned} \gamma_t &= -b_1 * Ft_x + c_1 Tt_z, \\ \beta_t &= b_1 * Ft_z + c_1 Tt_x, \end{aligned} \quad (18)$$

$$\begin{aligned} a_1 &= \frac{L^3}{3EI}, \\ b_1 &= \frac{L^2}{2EI}, \\ c_1 &= \frac{L}{EI}, \end{aligned} \quad (19)$$

Conversely, after some algebraic manipulations, the forces and torques acting on top can be written as follows:

$$\begin{aligned} Ft_x &= \frac{12EI}{L^3}w_x + \frac{6EI}{L^2}\gamma_t, \\ Ft_z &= \frac{12EI}{L^3}w_z - \frac{6EI}{L^2}\beta_t, \\ Tt_x &= -\frac{6EI}{L^2}w_z + \frac{4EI}{L}\beta_t, \\ Tt_z &= \frac{6EI}{L^2}w_x + \frac{4EI}{L}\gamma_t, \end{aligned} \quad (20)$$

The same idea is used for torsion and axial loadings,

$$Tt_y = \frac{GJ}{L}\alpha_t, \quad (21)$$

and

$$Ft_y = \frac{E * A}{L}w_y. \quad (22)$$

If the nacelle is fixed on top of the column, point *A*, the vectors force and torques have the same module but opposite directions. Besides, the angles and displacements of the nacelle and the column at the top must be the same, so

$$\begin{aligned} FnR_x &= -Ft_x, \\ TnR_x &= -Tt_x, \\ FnR_z &= -Ft_z, \\ TnR_z &= -Tt_z, \\ FnR_y &= -Ft_y, \\ TnR_y &= -Tt_y. \end{aligned} \quad (23)$$

Also,

$$\begin{aligned} \gamma_t &= \gamma, \\ \alpha_t &= \alpha, \\ \beta_t &= \beta, \end{aligned} \quad (24)$$

and

$$\begin{aligned} w_x &= u_x, \\ w_y &= u_y, \\ w_z &= u_z. \end{aligned} \quad (25)$$

Equations 23, 24 and 25 permit the substitution of the equations 20, 21 and 22 in the system of equations presented in 16. This is made by adding the coefficients that multiply the rotations and displacements, in equations previously mentioned, to the respective elements from the stiffness matrix in equation 16. Then, one has the motion of the turbine with the new condition imposed by the presence of the tower. No damping is considered here, although, it is present in real cases due mainly to the air action over the moving parts of the turbine.

5 SYSTEM UNDER RANDOM ANALYSIS

In this work some simplifications are imposed in order to make the simulations simpler and they will be presented along the text. It is considered that a mean wind velocity (U) of about 60 km/h (~ 22.2 m/s) is crossing the plane of rotation. It is asymmetric such that causes a variable deterministic torque which is considered as oscillating with the frequency of the rotor. Superposed to this, there is a random torque of magnitude which depends on the random behavior of the wind in the surroundings of the blade. This oscillation is estimated as having a normal distribution with null mean and standard deviation of $U_w = 2.2$ m/s (or about 10% of the nominal wind velocity). It is also considered that this value does not vary with the angular position of the blades.

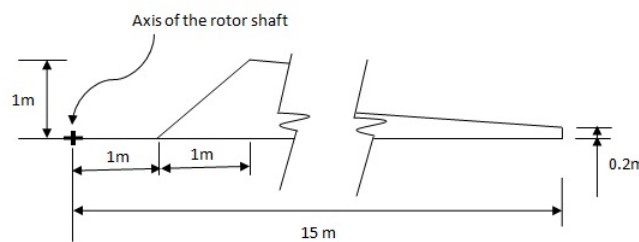


Figure 11: Blade considered

Description	Symbol	Values	Unit
Nominal rotor speed	Ω	6.0214	rad/s
Distance from point A to G	dn_1	0.513	$[m]$
Distance from point A to C	dn_2	2.388	$[m]$
Nacelle inertia - roll	In_x	26453	$[kgm^2]$
Nacelle inertia - yaw	In_y	26453	$[kgm^2]$
Nacelle inertia - pitch	In_z	26453	$[kgm^2]$
Rotor inertia - roll	Ih_x	22050	$[kgm^2]$
Rotor inertia - yaw	Ih_y	30	$[kgm^2]$
Rotor inertia - pitch	Ih_z	22070	$[kgm^2]$
Nominal Power	P_w	500	$[MW]$
Rotor rotational stiffness	Kh_ξ	$4.350e8$	$[Nms/rad]$
Rotor rotational dumping	Dh_ξ	$4.350e5$	$[Nms/rad]$
Nacelle mass	m_n	10000	$[kg]$
Rotor mass	m_h	2150	$[kg]$
Eccentricity	e	0.01	$[m]$
Rotor radius	R	15	$[m]$
Tower height (Hub)	L	29	$[m]$
Shaft diameter	D_s	0.2	$[m]$
Shaft thickness	t_s	0.02	$[m]$

Table 1: Data from the turbine

The wind rotates the rotor with an average in-plane torque that is a resultant of the components of the lift and drag forces. It was supposed that the power in steady state is $P_w = 500$ KW

and rotation is $\Omega = 6.0214 \text{ rad/s}$. In Table 1 it is presented some important system parameters used in the simulations. Then, the average in-plane torque is:

$$Tw_{in} = \frac{P_w}{\Omega} = \frac{500000 \text{ W}}{6.0214 \text{ rad/s}} = 83037 \text{ Nm} \quad (26)$$

This torque is due to the resultant of the components of the lift and drag forces projected in the rotation plane, along of the length of the blades. The resultant in-plane force is, by hypothesis, null. In out-plane, the wind causes forces, though. This force will not be calculated here and will be estimated to be ten times the value of force component of a binary equivalent to the torque Tw_{in} separated by a distance of 6 m. This force is considered deterministic. So,

$$Fw_{out} = 10 * \frac{Tb_{in}}{r_F} = \frac{830370 \text{ Nm}}{6 \text{ m}} = 138400 \text{ N} \quad (27)$$

The model is able to consider that there is a small fluctuation in torque Tw_{in} of random nature with standard deviation of about $10\%Tw_{in}$ with normal distribution,

$$\Delta Tw_{in} = 8304 \text{ Nm} \quad (28)$$

To calculate the fluctuating forces using the equations 2, 3 and 4, the geometrical characteristics of the blade must be known. The simplified blade is presented in Figure 11. It is formed by two simple geometric figures: one triangular and other trapezoidal. With these informations it is possible to obtain the function $c(r)$ and then the parameters, forces and torques presented in equations 2 and 3.

Then, after integration process, one obtains

$$m_{\xi_T} = 12860 \text{ m}^5. \quad (29)$$

If one considers the oscillation of the velocity independent of position in space r and that $\rho_{air} = 1.225 \text{ kg/m}^3$, after integration,

$$\Delta Fw_{out} = 2876 U_w, \quad (30)$$

and

$$\Delta Tw_{out} = 26930 U_w - (297932 \dot{\xi} + 1793969 \xi \tan(\delta_3)), \quad (31)$$

The first term in the right side of equation 31 is random because it is a function of U_w . The second term in the right side is dependent on the variable ξ which is the degree of freedom associated to the teetering movement. This term must be included in the damping and stiffness matrices in equation 16. So, the contribution of the fluctuating out-plane torque ΔTw_{out} to external loading vector is just $\Delta Tw_{out} = 26930 U_w$.

5.1 Simulations

The model was formulated under the conditions discussed above and a code was written in MatLab. The results of the simulations are presented below. The fluctuating wind velocities were considered as having normal probability density function with standard deviation equal to 2.2 m/s (10% of the mean wind velocity). The in plane torque ΔTw_{in} is also considered random with normal probability density function with standard deviation equal to 10% of ΔTw_{in} . The tower is built from a tube of steel ($E = 210 \text{ GPa}$ and $G = 80 \text{ GPa}$) with mean radius $r_t = 1 \text{ m}$ and thickness $t_t = 15 \text{ mm}$. It is assumed that the blades were mounted with a small unbalance of

0.01m. The system starts from a resting state with the blades in vertical position. The movement happens suddenly: the gravity and wind loading start to work and the blades start to rotate. The analysis is performed for 1.5 s, or about a rotation of 3π . Four spots (or sections) were chosen for analysis: at the hub, section containing the point C, at the connection nacelle/tower (section containing the point A), at the half height of the tower (15 m) and at the base (point O), as presented in Figure 12. After performing 100 trials for random analysis, the results in time for forces, displacements, angles and stresses were obtained (mean values).

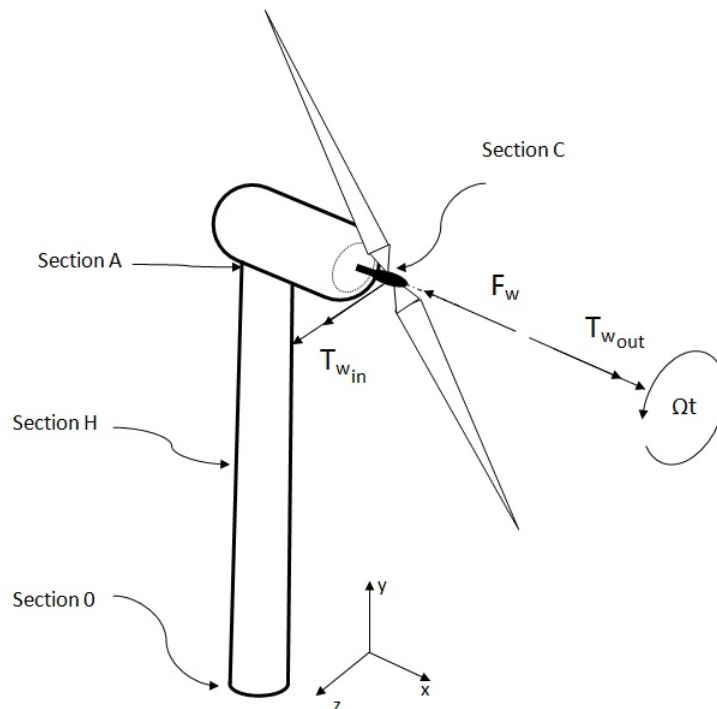
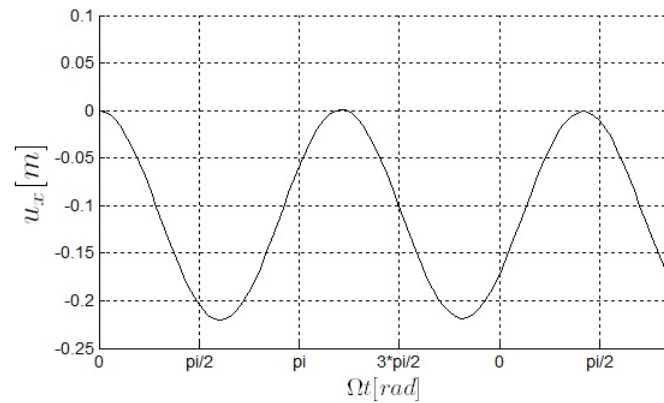
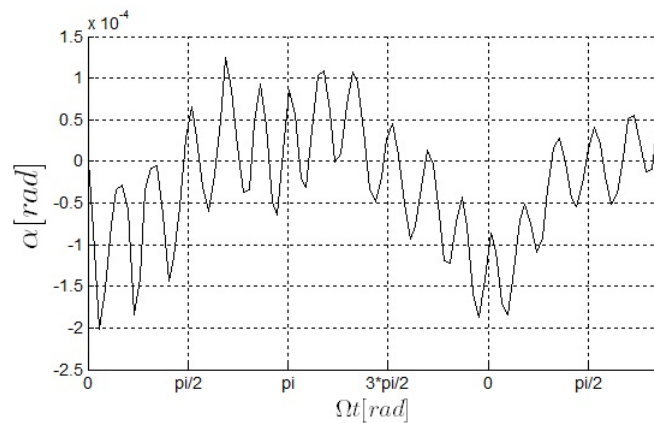


Figure 12: Loads due to wind action

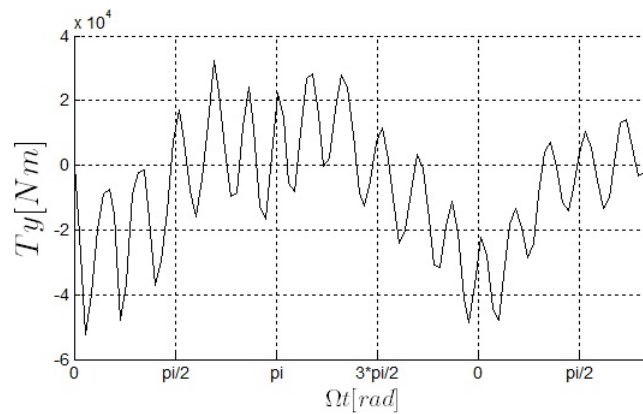
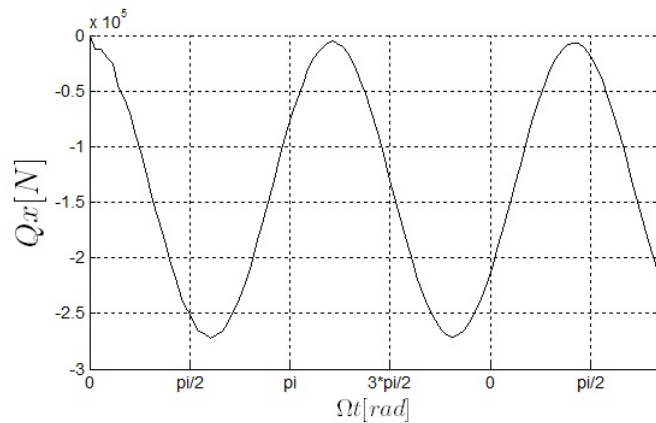
5.1.1 Displacements and rotations

The results for the average displacements in x is shown in Figure 13 and the angular movement α about y direction in Figure 14. As the force acts in x direction, this displacement is quite large in this direction and oscillates in a negative point of equilibrium. It is observed that the nacelle twists with a negative angle α at the beginning of the analysis. This happens because the resultant torque due to the weight of the nacelle/rotor and the wind force in x direction F_w causes a positive increment in angle γ (rotation about z axis). This causes a variation in the quantity of movement of the nacelle/rotor in direction z positive so the nacelle rotates in a angle α negative.

Figure 13: Displacement u_x Figure 14: Angle α

5.1.2 Torques and forces

Results for the average torque and shear force in y and x directions, respectively, are presented in Figure 15 and 16. The torque component T_y at the beginning of the analysis is negative, as expected considering the discussed above and is identical to that presented in Figure 14 but scaled. The graph in Figure 16 is also coherent with that of Figure 13.

Figure 15: Torque T_y Figure 16: Shear force Q_x at the top

5.1.3 Stress evaluation

The stresses in the four points of interest are shown below where the first graphs show the Mises stress at the point of maximum tractive stress which occurs at the border of the section. As the structure evolves in time, the point of the maximum Mises stress changes its position in the section. Except for in the hub stress analysis, the second graph gives the angle in the section (measured relative to axis z) where the maximum tractive stress happens (see Figure 17).

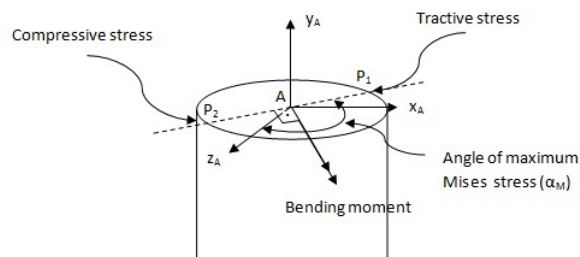


Figure 17: Angle of maximum Mises stress

a - Shaft stress analysis

For simulation of the shaft it was considered that it is a hollow cylindrical bar of a mean radius of 200 mm and a thickness of 20 mm. The combination of shear stress caused by torque in- and out-plane was performed by calculating the Mises stress. The results are shown in Figure 18.

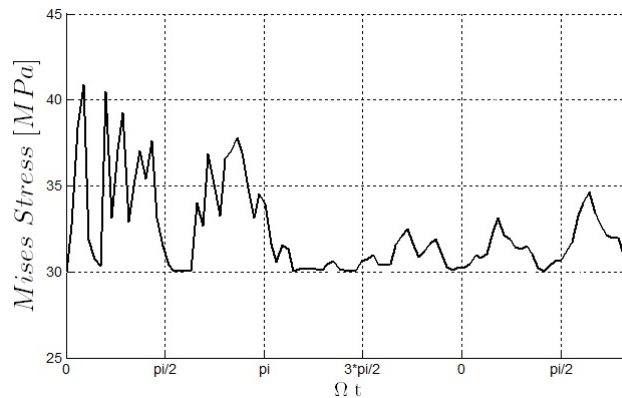


Figure 18: Mises stress in the connection with hub

b - Stress at the tower top

The Mises stresses at the top of the tower (section containing the point A) are presented in Figure 19. The angular position of the occurrence of maximum stress is presented in Figure 20.

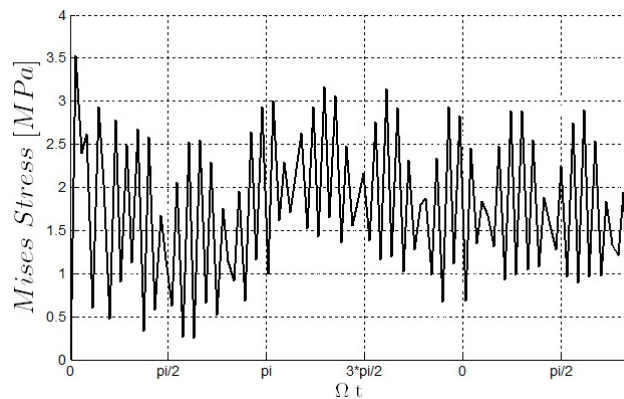
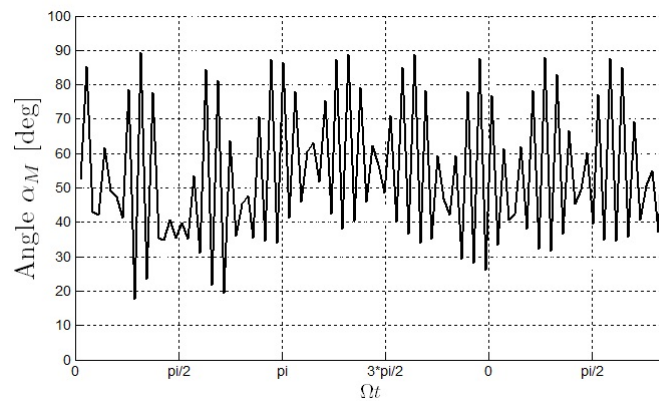


Figure 19: Mises stress in section A

Figure 20: Angle α_M at section A

c - Stress at a section 15m from bottom up

The Mises stresses at a height of 15m is presented in Figure 21. The angular position of the occurrence of the maximum stress is presented in Figure 22.

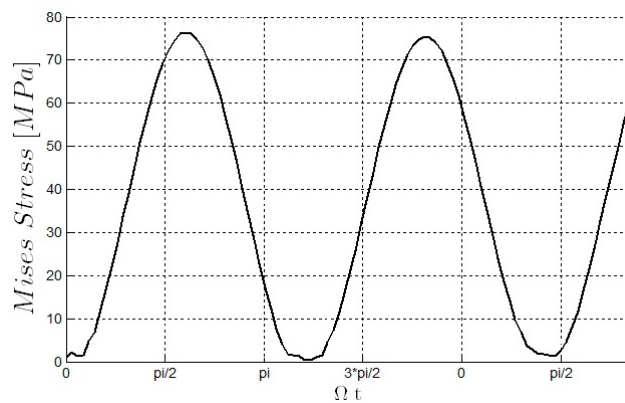
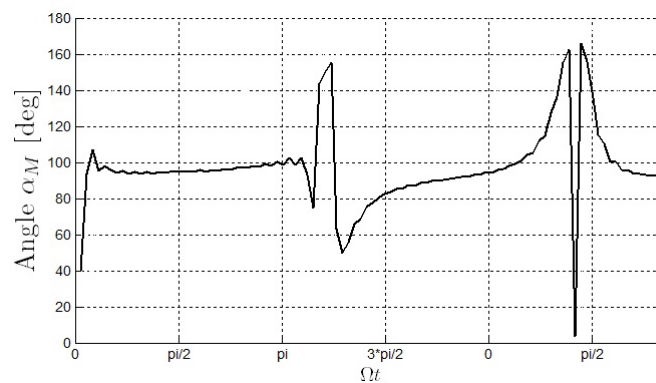


Figure 21: Mises stress at 15 m from the base

Figure 22: Angle α_M at 15 m

d - Stress at the base

The Mises stresses at the base of the tower is presented in the Figure 23. The angular position of the point of maximum stress is presented in Figure 24.

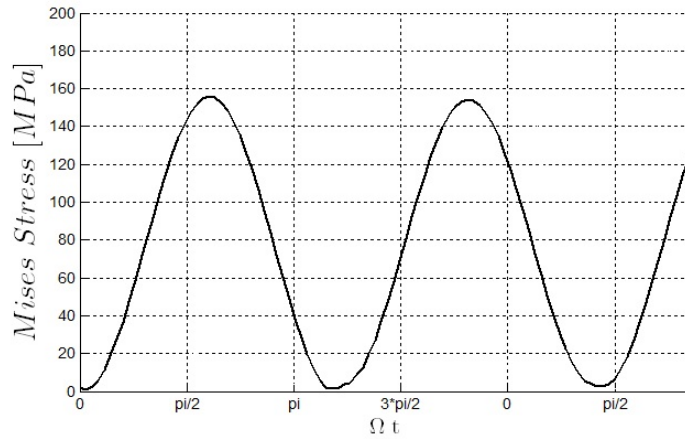


Figure 23: Mises stress at the base

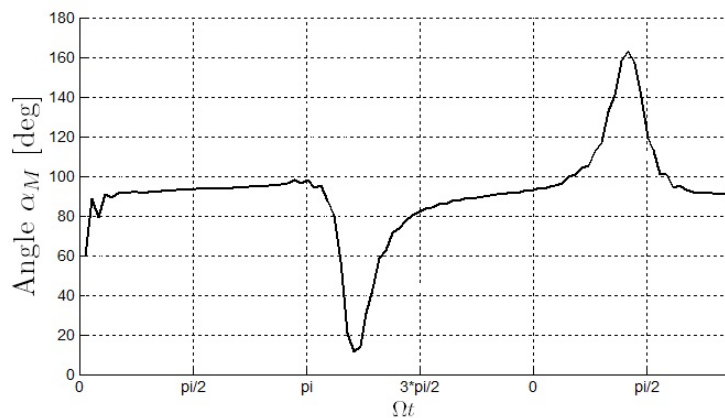
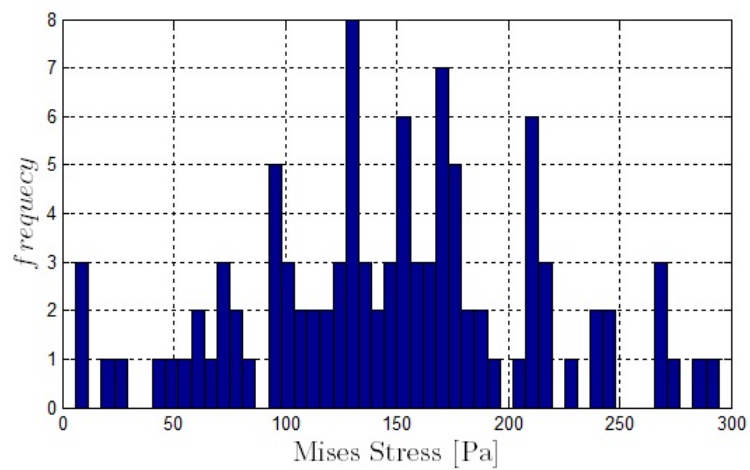
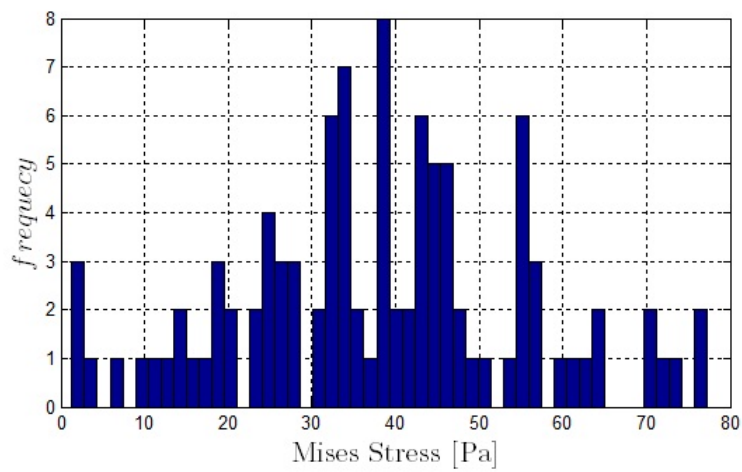
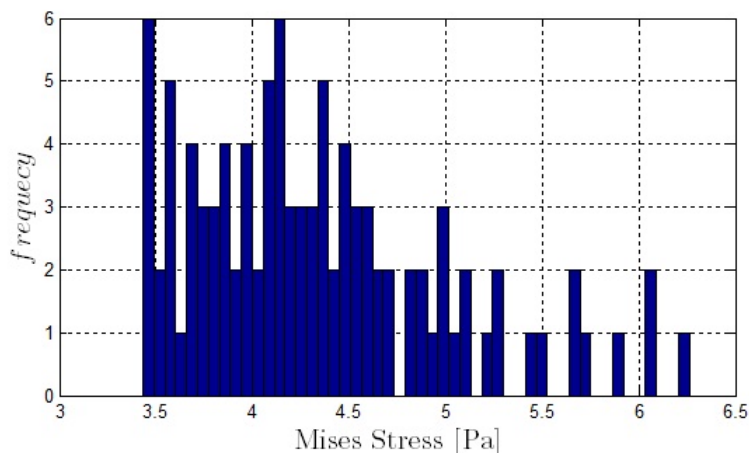


Figure 24: Angle α_M at the base

For this case, histograms were made for three positions of the rotor (namely, $\pi/2$, π and $5\pi/4$). They are presented below.

Figure 25: Point $\Omega t = \pi/2$ Figure 26: Point $\Omega t = \pi/2$

Figure 27: Point $\Omega t = 5\pi/4$

6 CONCLUSIONS

In this work, the equations for the motion of a nacelle and a rotor installed on a tower assumed Bernoulli-Euler type without inertial effects, were derived using directly the Euler and Newton laws. Using a simple formulation for the wind loading, deterministic and random loads simulating the wind were applied and results were obtained for stresses in four important points of the structure. The blades deform under the wind and vibrate, interacting with the nacelle and consequently with the tower. The formulation obtained considered the blades as rigid bodies with teetering motion. The approach was always to consider the bodies moving under small rotations and displacements, except for the in-plane motion of the rotor. The behavior of the structure under the action of wind loads depends on the individual behavior of the blades, nacelle and tower but their motions are coupled, and the formulation takes this in consideration. Although not considering large rotor angular velocities variations, the model permits small in-plane perturbations by considering that this just affects the rotations about x axis. This permits to model the interaction between the nacelle and rotor, that means it is possible to consider the effect of the in-plane torque (caused by wind) in the motion of the nacelle. The limitation imposed in the tower formulation, permits only analysis for sufficiently small motion. Other important limitation is that this model is valid for low frequencies. This is clearly an important limitation since turbines are submitted to wind regime and the excitations can happen in high frequencies too (Veldkamp (2006)). It can be useful to help in performing a fast analysis in the structure to obtain an approximation of the solution. Then, based on the data obtained, a more complete analysis can be performed, with lower cost, considering the information acquired. As the eolic systems grow in size, the costs to design, mount and operate them increase so that more comprehensive and complex models must be developed for incorporate design details and ensure reliability and safety for such structures keeping the design economically possible. A more complete model is being developed to take in consideration large variations in nacelle yaw, row and pitch angle and similarly to the rotor dynamics, which will permit a realistic transient evaluation. FEM in conjunction with modal analysis seems to be an interesting line to follow to study the assemble of tower and nacelle and this simple formulation is the basis for further investigations on the behavior of eolic structures.

REFERENCES

- Andersen B. *A comparison of two and three bladed floating wind turbines*. Ph.D. thesis, The University of Toledo-Ohio, US, 2010.
- Burton T., Jenkins N., Sharpe D., and Bossanyi E. *Wind Energy Handbook*. John Wiley and Sons, Ltd, Chichester West Sussex, England, 2001.
- Gasch R. T.J. *Windkraftanlage 6th Ed*. GWV Fachverlage, GmbH, Wiesbade, 2010.
- Hansen M.O.L. *Aerodynamics of Windturbines 2nd Ed*. Sterling, London, 2008.
- Kane T. R. L.D.A. *Dynamics: Theory and Applications*. McGraw-Hill Publishing Company, New York, 1985.
- Mikkelsen R. *Actuator Disc Methods Applied to Wind Turbines*. Ph.D. thesis, Technical University of Denmark DK-2800 Lyngby, Denmark, 2003.
- Ramirez J. *Reliability Assess. and Reliab.-Based Inspe. and Maint. of Offshore Wind Turbines*. Ph.D. thesis, Aalborg University, 2010.
- Shigley J.E. *Mechanical Engineering Design-1st Ed*. ABL, New York, 1978.
- Spiegelberg B. *Dynamical Analysis of the Windflow 500 Wind Turbine*. Ph.D. thesis, Technische Universität Darmstadt, 2011.
- Veldkamp H.F. *A Probabilistic Approach to Wind Turbine Fatigue Design*. Ph.D. thesis, Technical University of Delft, 2006.

7 ANNEX A

Matrix determination for nacelle and rotor supported by dumpers and springs. To formulate the effect of the tower, the matrix elements from the beam formulation must be inserted in the stiffness matrix.

a - Rotor angular position $\omega = \Omega * t$

b - Parameters

$$Sin = \sin(\omega)$$

$$Cos = \cos(\omega)$$

$$SinQuad = (\sin(\omega))^2$$

$$CosQuad = (\cos(\omega))^2$$

$$CosSin = Cos Sin$$

$$ct_1 = m_h e Sin$$

$$ct_2 = m_h e Cos$$

$$ct_3 = m_h e$$

$$ct_5 = ct_3 e$$

$$m_{tot} = m_h + m_n$$

$$ct_4 = (m_h dn_2 + m_n dn_1)$$

$$ct_6 = (Ih_z - Ih_y)$$

$$ct_7 = (Ih_x - Ih_y)$$

$$ct_8 = Omega Cos$$

$$ct_9 = Omega Sin$$

$$ct_{10} = Omega CosQuad$$

$$ct_{12} = Omega CosSin$$

$$ct_{13} = Omega SinQuad$$

c - Mass Matrix [M]

$$[M]_{11} = In_x$$

$$[M]_{22} = In_y + m_n(dn_1)^2 + m_h(dn_2)^2 + Ih_y CosQuad + (Ih_z + ct_5) SinQuad$$

$$\begin{aligned}
[M]_{23} &= -(ct_6 + ct_5)CosSin \\
[M]_{24} &= (-Ih_z - ct_5)Sin \quad [M]_{27} = -m_h dn_2 \\
[M]_{32} &= -(ct_6 + ct_5)CosSin \\
[M]_{33} &= In_z + m_n(dn_1)^2 + m_h(dn_2)^2 + (Ih_z + ct_5)CosQuad + Ih_y SinQuad \\
[M]_{34} &= (Ih_z + ct_5)Cos \\
[M]_{36} &= m_h dn_2 \\
[M]_{42} &= -(Ih_z + ct_5)Sin \\
[M]_{43} &= (Ih_z + ct_5)Cos \\
[M]_{44} &= Ih_z + ct_5 \\
[M]_{46} &= -ct_3 \\
[M]_{55} &= (m_t ot) \\
[M]_{63} &= ct_4 \\
[M]_{73} &= -(ct_4) \\
[M]_{77} &= (m_t ot)
\end{aligned}$$

d - Dumping matrix

$$\begin{aligned}
[D]_{11} &= Dn_\beta \quad [D]_{22} = Dn_\alpha + (ct_6 + ct_5)ct_{12} \\
[D]_{23} &= (ct_6 + ct_5)ct_{13} - (Ih_z - Ih_x)\Omega \\
[D]_{24} &= (ct_7 - Ih_z)ct_8 \\
[D]_{32} &= -(ct_6 + ct_5)ct_{10} + (Ih_z - Ih_x)\Omega \\
[D]_{33} &= Dn_\gamma - (ct_6 ct_{12}) + \chi Sin \\
[D]_{34} &= -Ih_z ct_9 \\
[D]_{42} &= -(ct_7 + Ih_z + 2ct_5)ct_8 \\
[D]_{43} &= -(ct_7 + Ih_z + 2ct_5)ct_9 \\
[D]_{44} &= Dh_\xi + \chi\Omega \\
[D]_{55} &= Dn_x \\
[D]_{66} &= Dn_y \\
[D]_{77} &= Dn_z
\end{aligned}$$

e - Stiffness matrix

$$\begin{aligned}
[K]_{11} &= Kn_\beta \\
[K]_{22} &= Kn_\alpha \\
[K]_{24} &= -Sin\Omega^2 * (ct_7 + \chi * tan(Delta3)) \\
[K]_{33} &= Kn_\gamma \\
[K]_{34} &= Cos\Omega^2 * (ct_7 + \chi * tan(Delta3)) \\
[K]_{44} &= Kh_{xi} + (ct_7)\Omega^2 \\
[K]_{55} &= Kn_x \\
[K]_{66} &= Kn_y \\
[K]_{77} &= Kn_z
\end{aligned}$$